



# Prediction of effective thermomechanical behavior of shape memory polymer composite with micro-damage interface

Xiaozhou Xin<sup>a</sup>, Liwu Liu<sup>a,\*</sup>, Yanju Liu<sup>a</sup>, Jinsong Leng<sup>b,\*\*</sup>

<sup>a</sup> Department of Astronautical Science and Mechanics, Harbin Institute of Technology (HIT), P.O. Box 301, No. 92 West Dazhi Street, Harbin, 150001, People's Republic of China

<sup>b</sup> Center for Composite Materials and Structures, Harbin Institute of Technology (HIT), No.2 Yikuang Street, P.O. Box 3011, Harbin, 150080, People's Republic of China

## ARTICLE INFO

### Keywords:

Shape memory polymer composite  
Thermomechanical properties  
Micromechanics  
Particle reinforced composite

## ABSTRACT

Shape memory polymer composite (SMPC) not only retains the unique stimuli-responsive ability of shape memory polymer (SMP), but also enhances the thermomechanical behavior of SMP. Although relatively complete thermal prediction models of SMPC have been established, the displacement jump due to interface damage has hardly been considered in these models. In this work, the thermomechanical constitutive model of SMPC considering the interface and micro-damage behavior is derived. The effective mechanical behaviors of SMPC under different temperatures and damage conditions are deduced by modifying Eshelby tensor and Mori-Tanaka method. Taking MWCNT/SMP composite as an example, the reliability of the model is verified by the thermo-mechanical coupling tests. More importantly, the model can also predict other reinforced types of SMPC by changing the configuration parameters and physical properties of the reinforcement phase.

## 1. Introduction

Shape memory polymer (SMP) has the ability of maintaining a deformed temporary shape and recovering to its original shape under stimuli (such as heat, light, magnetism, electricity) [1–4]. Due to its high strain recovery (~400%), low cost, and biocompatibility, SMP has attracted a wide range of research interests, including aerospace, biomedicine etc. [5–9]. By introducing reinforcement phase into SMP, the thermomechanical properties of shape memory polymer composites (SMPC) can be improved to meet the complex service environment [10, 11].

It is necessary to establish effective mechanical models to predict its thermomechanical properties before engineering applications. According to the thermodynamic properties of SMP, it can be divided into frozen and active phase. Based on viscoelastic theory and phase transition theory, the constitutive model of SMP can be established [12]. Different from the traditional composite, the effective mechanical properties of SMPC depend on the mechanical properties and orientation of the reinforcement phase, as well as the viscoelasticity of SMP [13–19]. In addition, the interaction between SMP and reinforcement

phase should also be considered in the model. However, most of the developed prediction models are limited by the idealized assumption: the inclusions are in ideal contact with SMP. In fact, SMPC form an interface layer through physical interaction and chemical reaction during the curing process [20,21]. SMPC experiences large deformation at high temperature, and the interface shear stress may cause damage, which affects the thermomechanical performance and service life of SMPC.

In this work, a new model describing the change of the interface phase properties along the radial gradient was established, and the micromechanical model of the viscoelastic interface with micro-damage was derived. The displacement jump caused by interface damage was investigated by modifying Eshelby tensor. The effective relaxation modulus of SMPC with single inclusion at different temperatures was calculated by Mori-Tanaka (M-T) method. The reliability of the developed model was verified by relaxation test, isothermal cycle test, and thermomechanical programming test of SMPC. The effect of micro-damage on effective mechanical properties and shape memory performance was also investigated.

\* Corresponding author. Department of Astronautical Science and Mechanics, Harbin Institute of Technology (HIT), P.O. Box 301, No. 92 West Dazhi Street, Harbin, 150001, People's Republic of China.

\*\* Corresponding author. Center for Composite Materials and Structures, Harbin Institute of Technology (HIT), No.2 Yikuang Street, P.O. Box 3011, Harbin, 150080, People's Republic of China.

E-mail addresses: [liulw@hit.edu.cn](mailto:liulw@hit.edu.cn) (L. Liu), [lengjs@hit.edu.cn](mailto:lengjs@hit.edu.cn) (J. Leng).

<https://doi.org/10.1016/j.coco.2021.100727>

Received 4 February 2021; Received in revised form 8 March 2021; Accepted 16 March 2021

Available online 27 March 2021

2452-2139/© 2021 Published by Elsevier Ltd.

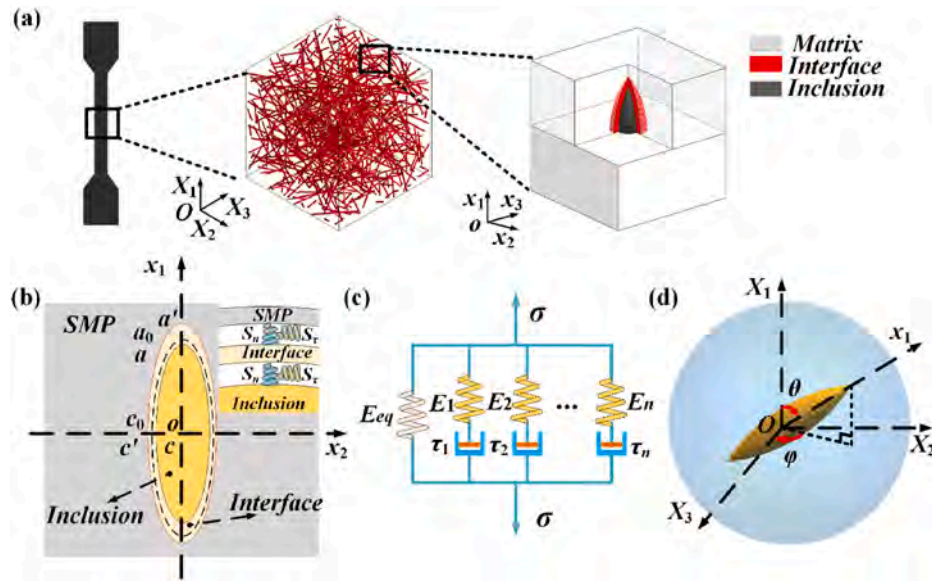


**Fig. 1.** (a) SMPC specimen (left), the inclusions 3D randomly distributed in SMP (middle), and RVE with a single ellipsoid inclusion (right). (b) Schematic diagram of micromechanical model. The dotted line is the geometric dimension of the original inclusion. (c) The GMM model. (d) The distribution direction of inclusion in  $O-X_1X_2X_3$  was described by  $O-\theta\phi r$ .

## 2. Materials and method

The two types of epoxy-based thermosetting shape memory polymer ( $T_g = 170.07$  and  $188.00$  °C) used in this work were prepared by the group of Prof. Jinsong Leng of Harbin Institute of Technology. Multi-walled carbon nanotubes (MWCNT) with a diameter of 20–30 nm was purchased from Chengdu Institute of Organic Chemistry. The blend containing 2 wt% MWCNT and SMP was mechanically stirred at 25 °C for 30 min and oscillated in an ultrasonic bath for 15 min to make MWCNT evenly dispersed in SMP.

The thermal dynamic mechanical properties of SMP was tested at a constant frequency of 1 Hz at a rate of  $2.5$  °C  $\text{min}^{-1}$  by DMA Q800.

The stress relaxation behaviors were tested by the ZWICK-010 tensile machine with an environmental chamber in accordance with standard ASTM D638.

The isothermal cyclic behavior of SMPC was investigated by ZWICK-010 tensile machine. The sample was kept at 150 °C for 15 min to achieve thermal equilibrium, then the sample was stretched by 2.8% (engineering strain) at a loading rate of  $2$  mm  $\text{min}^{-1}$ . When reached the target deformation, the sample was immediately unloaded at a rate of  $2$  mm  $\text{min}^{-1}$  until the stress reached 0 MPa.

## 3. Micromechanical model

Fig. 1a shows the 3D random distribution of ellipsoidal inclusions with an outer surface dimension ( $a_0, c_0, c_0$ ) in SMP. The slenderness ratio ( $\rho = a_0/c_0$ ) was used to describe the configuration of the inclusions. In local coordinate system ( $o-x_1x_2x_3$ ), the representative volume element (RVE) with a single ellipsoid inclusion was established, which consisted of SMP, interface, and ellipsoidal inclusion (Fig. 1b, Section-S1 and Section-S2 for details).

In this work, superscripts (0), (1), and (2) represented the reinforcement phase, interface phase, and SMP, respectively. It was assumed that the interfacial phase was composed of SMP and inclusion, and the content of the two phases changed in gradient. The ratio of the volume of the SMP at any point in the interface phase to the volume of the interface ( $g_{SMP}^{(1)}(r) = V_{SMP}^{(1)}(r)/V^{(1)}$ ) satisfied:

$$g_{SMP}^{(1)}(r) = \left(\frac{r-\zeta}{1-\zeta}\right)^\chi \exp\left[\left(\frac{r-\zeta}{1-\zeta}\right)^\chi - 1\right] \quad \zeta = \frac{a}{a'} = \frac{c}{c'} \quad (1)$$

where,  $r$  was the ratio of the radial dimension of any point to the outer surface of the interface,  $r \in [\zeta, 1]$ . The volume fraction of the inclusion at this point was  $g_{inclusion}^{(1)}(r) = 1 - g_{SMP}^{(1)}(r)$ .

Hooke's law was used to describe the deformation behavior of reinforcement phase. The generalized Maxwell model (GMM, Fig. 1c) was used to describe the viscoelastic behavior of SMP and homogenized SMPC. The stiffness of the interface was [22]:

$$\mathbf{L}^{(1)}(T, t, r) = \mathbf{L}^{(0)} - (\mathbf{L}^{(0)} - \mathbf{L}^{(2)}(T, t))g_{SMP}^{(1)}(r) \quad (2)$$

where,  $\mathbf{L}^{(i)}$  was the stiffness tensor of the  $i$  phase.

The discontinuous displacement of the interface was described by inserting the springs (Fig. 1b), and the boundary condition was [22]:

$$\Delta u_i = n_{ij}\sigma_{jk}n_k \quad n_{ij} = S_\tau\delta_{ij} + (S_n - S_\tau)n_in_j \quad (3)$$

where,  $S_n$  and  $S_\tau$  represented the compliance of normal and tangential springs respectively. The effective stiffness of the single inclusion in  $o-x_1x_2x_3$  can be obtained by M-T method [22].

$$\mathbf{L}_{uni}^{eff} = \left(\sum_{i=0}^2 f^{(i)}\mathbf{L}^{(i)}:\mathbf{A}^{(i)}\right) : \left[\sum_{i=0}^2 f^{(i)}\mathbf{A}^{(i)} + \sum_{i=0}^1 f^{(i)}\mathbf{H}:\mathbf{L}^{(i)}:\mathbf{A}^{(i)}\right]^{-1} \quad (4)$$

Obviously, the orientation of the inclusion with  $\rho \neq 1$  affected the effective properties of SMPC in the global coordinate system ( $O-X_1X_2X_3$ ). The spherical coordinate system ( $O-\theta\phi r$ ) was established to describe the direction of inclusions in the  $O-X_1X_2X_3$  (Fig. 1d). In particular, SMPC with the 3D random distribution of the inclusions can be regarded as isotropic material (Section-S4):

$$\mathbf{L}_{3D}^{eff} = \frac{1}{4\pi} \int_0^\pi \int_0^{2\pi} \bar{\mathbf{L}}^{eff} \sin\theta d\phi d\theta = (3K^{eff}, 2G^{eff}) \quad (5)$$

where,  $K^{eff} = \frac{1}{9}[4\alpha^{eff} + 2(\beta^{eff} + \beta^{eff'}) + \gamma^{eff}]$ ,  $G^{eff} = \frac{1}{15}[\alpha^{eff} - (\beta^{eff} + \beta^{eff'}) + \gamma^{eff} + 6(\theta^{eff} + \omega^{eff})]$ .  $K^{eff}$  and  $G^{eff}$  represent the bulk modulus and shear modulus of SMPC after homogenization, respectively.

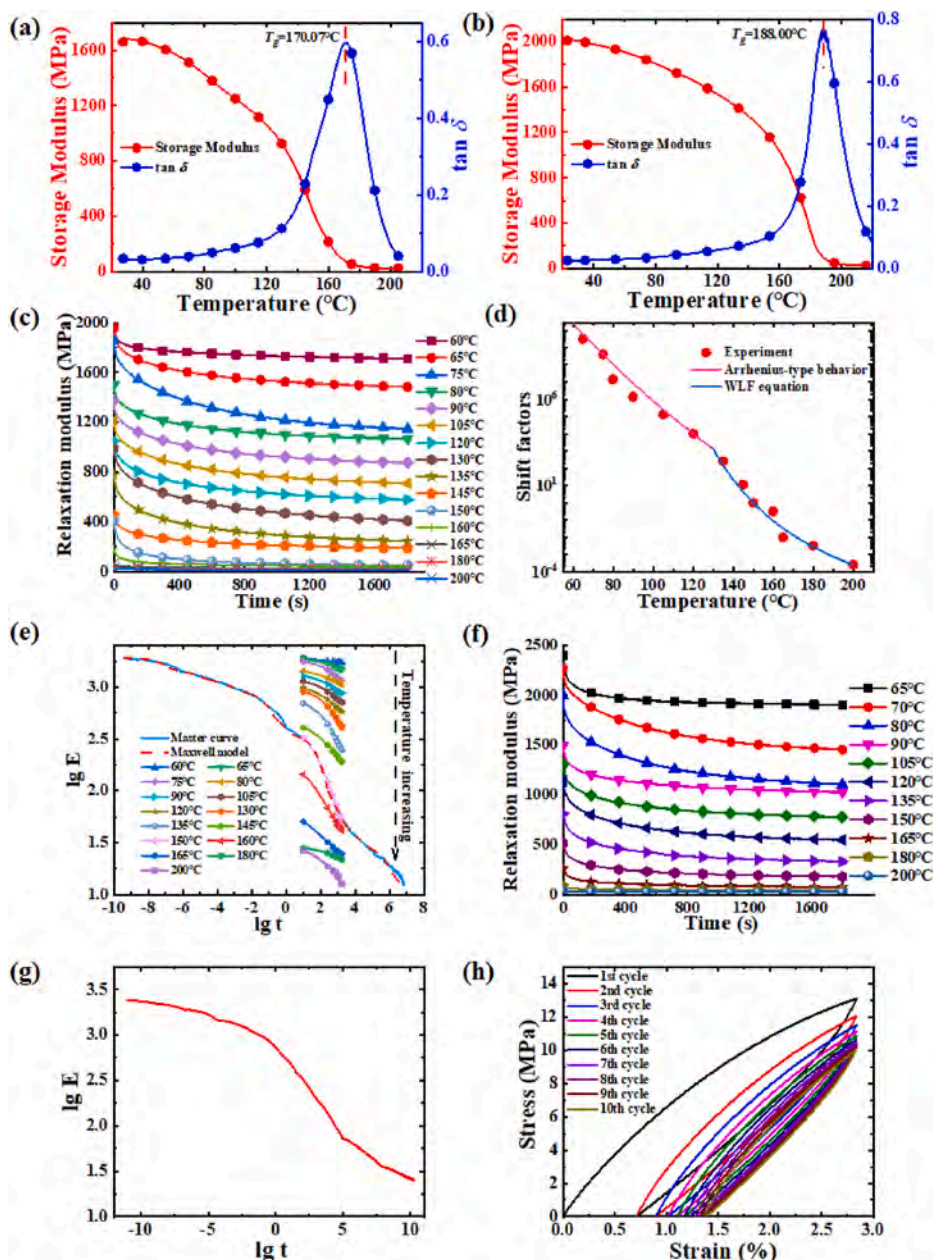


Fig. 2. (a)~(b) DMA test curve of SMP. (c) Stress relaxation behaviors of SMP. (d) The relationship between  $\alpha_T$  and temperature. (e) Comparison of relaxation master curve obtained by experiment and the GMM model. (f) Stress relaxation behavior of SMPC. (g) The relaxation master curve of SMPC. (h)  $\sigma$ - $\epsilon$  behavior of SMPC under cyclic loading.

## 4. Results

### 4.1. Experimental results

The glass transition temperature ( $T_g$ ) of two types of epoxy-based thermosetting SMP obtained from the  $\tan \delta$  curves were 170.07 and 188.00 °C (Fig. 2a and b). Here SMP with  $T_g = 170.07$  °C was used to prepare SMPC. The phase transformation (from the glassy phase to the rubbery phase) led to the decrease of the initial relaxation modulus with the increased temperature (Fig. 2c). Fig. 2d exhibits the time-temperature superposition (TTSP) shifting factor ( $\alpha_T$ ) as the function of temperature. Using the Williams-Landel-Ferry (WLF) equation (Eq. S(22)) and Arrhenius type behavior (Eq. S(23)) to fit the  $\alpha_T$  obtained from the TTSP, and the intersection of the two fitting curves is the shifting temperature ( $T_s$ ). When the temperature was higher and lower than  $T_s$ ,  $\alpha_T$  followed Eq. S(22) and Eq. S(23) respectively (Section-S5). The actual

relaxation behavior of SMP at 150 °C for a long time ( $T_{ref} = 150$  °C) was obtained by time-temperature equivalence principle (Fig. 2e). The GMM model can reproduce the master curve with high accuracy (Fig. 2e, Table S1).

Fig. 2f and g exhibit the relaxation modulus at different temperatures and the relaxation master curve of SMPC. Due to the introduction of MWCNT, SMPC had an increased initial relaxation modulus at each test temperature compared to the SMP. Fig. 2h reveals the stress-strain ( $\sigma$ - $\epsilon$ ) curve of SMPC at 150 °C for 10 loading cycles. The peak stress of each cycle decreased due to the softening of SMPC. The residual strain was observed after the first cycle ( $\sim 0.71\%$ ) and increased with the increase of the number of cycles. After the 8th cycle, the residual strain of SMPC tended to be saturated  $\sim 1.39\%$ .

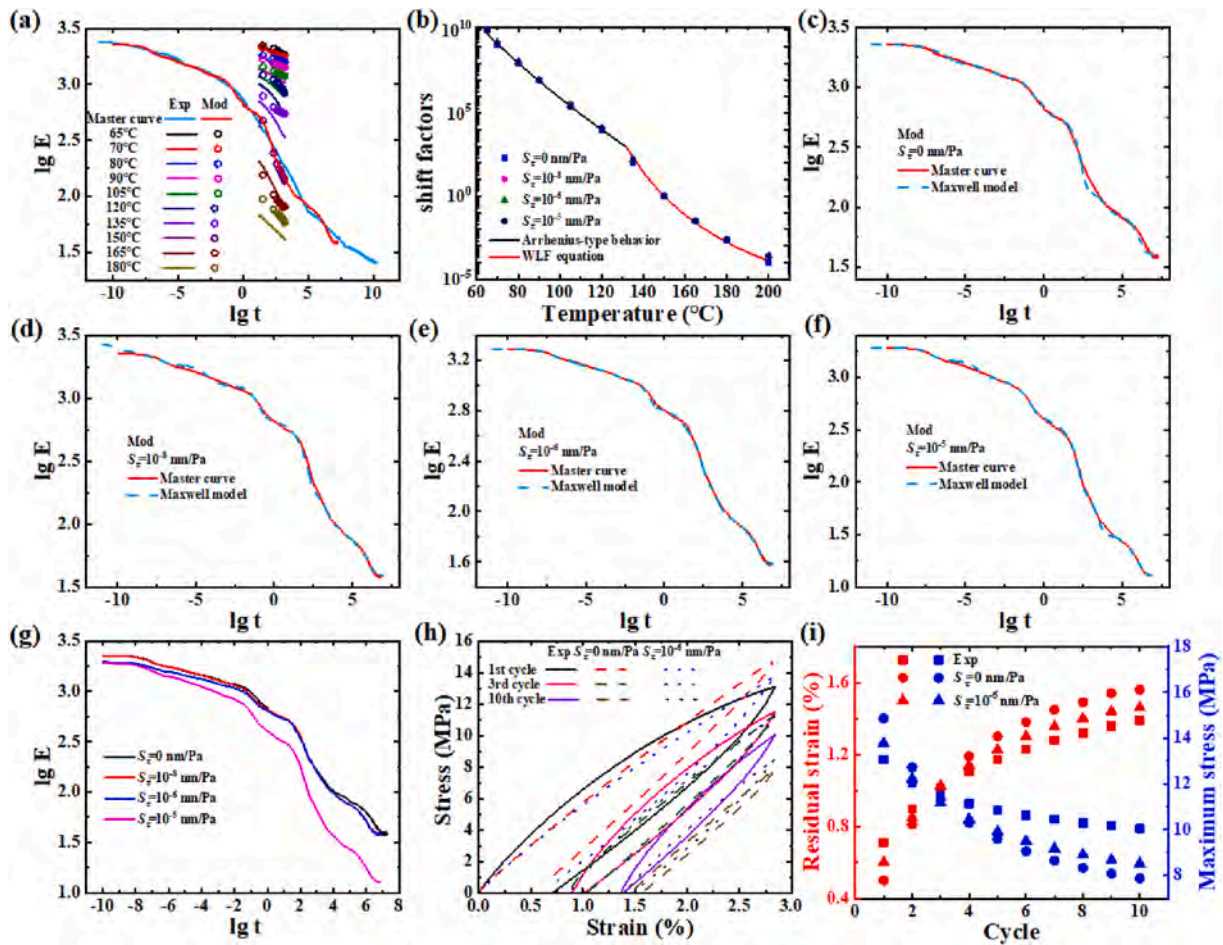


Fig. 3. (a) Comparison of the experimental and the prediction results. (b) The relationship between  $\alpha_T$  and temperature. Comparison of the master curve obtained by the micromechanical model and the GMM model under different damage (c)  $S_\tau = 0$  (d)  $10^{-8}$  (e)  $10^{-6}$  (f)  $10^{-5}$  nm/Pa. (g) Comparison of the master curves of different damage obtained by micromechanical model. Experimental and predicted comparison of (h)  $\sigma$ - $\varepsilon$ , (i) residual strain and maximum stress of SMPC under cyclic loading.

#### 4.2. Prediction results

Fig. 3a shows the comparison of the model prediction (point) and experiment (line) of the relaxation modulus and the master curve ( $T_{ref} = 150^\circ\text{C}$ ) of SMPC at  $S_\tau = 0$  nm/Pa (Table S2). The predicted results were in good agreement with the experiment at each temperature. The parameters were obtained by extracting the  $\alpha_T$  at different temperatures and performing non-linear fitting (Fig. 3b). The predicted values of the master curves of the SMPC after homogenization with different interface damage parameters were obtained (solid line in Fig. 3c~f), which were accurately reproduced by the GMM model (dashed line in Fig. 3c~f). Fig. 3g summarizes the master curves with four different damage parameters ( $S_\tau = 0$  nm/Pa,  $10^{-8}$  nm/Pa,  $10^{-6}$  nm/Pa and  $10^{-5}$  nm/Pa), which more clearly showed the influence of interface damage on the master curve. The relaxation modulus of SMPC decreased with the increase of damage, which was more obvious when  $T > T_g$ .

The  $\sigma$ - $\varepsilon$  behaviors of SMPC with different interface damage under cyclic tensile load were investigated. Fig. 3h exhibits the comparison result between the experimental and the theoretical value of the  $\sigma$ - $\varepsilon$  at  $150^\circ\text{C}$ . The evolution of the residual strain and maximum stress of SMPC with the increase of the number of cycles is shown in Fig. 3i. As the number of cycles increased, the residual strain increased from  $\sim 0.6\%$  to  $\sim 1.6\%$ , and the maximum stress decreased from  $\sim 14$  MPa to  $\sim 8$  MPa. In addition, after several loading cycles, the elasticity of SMPC tended to be stable due to the gradual stabilization of residual strain and maximum stress.

The shape memory cycle behavior of SMPC was investigated,

including stretching ( $T = 180^\circ\text{C}$ ), cooling, unloading, and free recovery. The comparison results between the predicted value and the previous work [14] in the process of shape memory programming is shown in Fig. 4. The experimental results were in good agreement with the prediction. The maximum stress of SMPC decreased with the increase of  $S_\tau$ . The shape fixation rate ( $R_f$ ) and shape recovery rate ( $R_r$ ) of SMPC were:

$$R_f = \frac{\varepsilon_u}{\varepsilon_p}, R_r = \frac{\varepsilon_p - \varepsilon_r}{\varepsilon_p} \quad (6)$$

where  $\varepsilon_p$  was the prescribed axial strain,  $\varepsilon_u$  was the strain after unloading, and  $\varepsilon_r$  was the axial strain of the specimen after recovery. The  $R_f$  of the experiment, FEM,  $S_\tau = 0$  nm/Pa,  $S_\tau = 10^{-6}$  nm/Pa,  $S_\tau = 10^{-5}$  nm/Pa were 87%, 76%, 99.33%, 98.57%, 98.02%, and  $R_r$  were 77%, 100%, 97.49%, 97.48%, 97.076%.

#### 5. Conclusion

In summary, the interface phase was inserted between SMP and inclusion phase, and a new model of  $g_{\text{matrix}}^{(1)}$  was proposed to describe the gradient change of mechanical properties of interfacial phase. The effective mechanical behavior of SMPC with different interface damages was deduced by micromechanical method. The reliability of the model was verified. The modulus of SMPC decreased due to interface damage, which was more obvious at  $T > T_g$ . The increase of interface damage led to the decrease of  $R_f$  and  $R_r$ . It was worth noting that the model can also predict the effective thermomechanical behavior of other reinforced

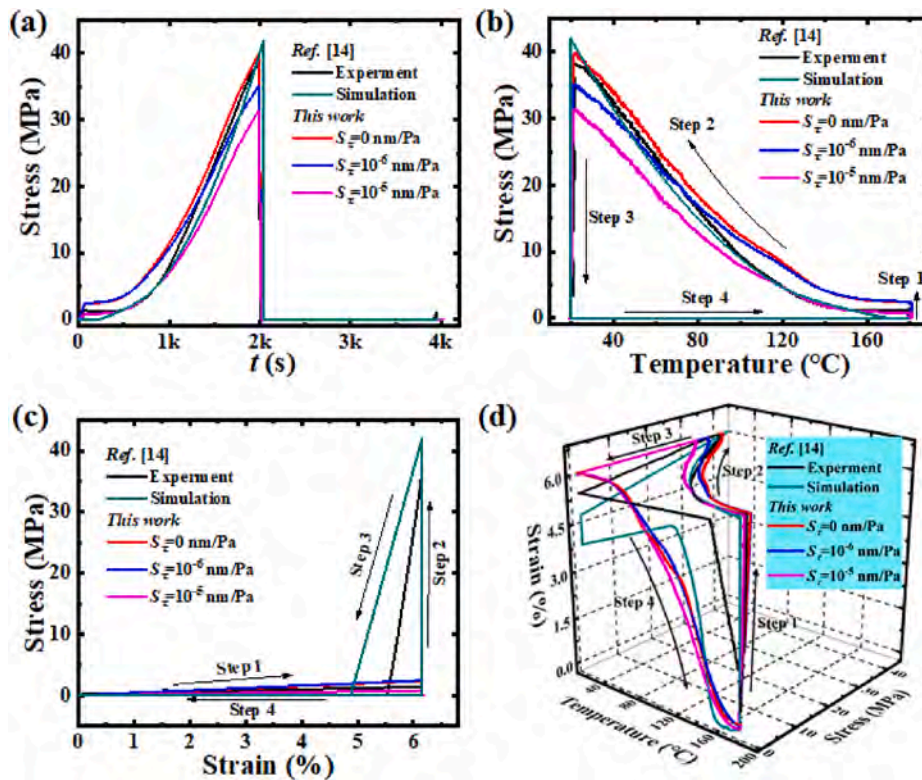


Fig. 4. Experimental and theoretical results of shape memory behavior.

forms of SMPC by changing slenderness ratio and stiffness tensor of the reinforcement phase.

#### CRedit authorship contribution statement

**Xiaozhou Xin:** Methodology, Writing – original draft. **Liwu Liu:** Data curation, Writing – review & editing. **Yanju Liu:** Investigation, Funding acquisition. **Jinsong Leng:** Supervision, Funding acquisition.

#### Declaration of competing interest

The authors declare that they have no known competing financial interests or personal relationships that could have appeared to influence the work reported in this paper.

#### Acknowledgments

The authors gratefully acknowledge the financial supports provided by the National Natural Science Foundation of China (Grant Nos. 11632005 and 11672086).

#### Appendix A. Supplementary data

Supplementary data to this article can be found online at <https://doi.org/10.1016/j.coco.2021.100727>.

#### References

- [1] T. Mu, L.W. Liu, X. Lan, Y.J. Liu, J.S. Leng, Shape memory polymers for composites, *Compos. Sci. Technol.* 160 (2018) 169–198.
- [2] W. Voit, T. Ware, R.R. Dasari, P. Smith, L. Danz, D. Simon, S. Barlow, S.R. Marder, K. Gall, High-strain shape-memory polymers, *Adv. Funct. Mater.* 20 (1) (2010) 162–171.
- [3] T. Xie, I.A. Rousseau, Facile tailoring of thermal transition temperatures of epoxy shape memory polymers, *Polymer* 50 (8) (2009) 1852–1856.
- [4] X.Z. Xin, L.W. Liu, Y.J. Liu, J.S. Leng, Mechanical models, structures, and applications of shape-memory polymers and their composites, *Acta Mech. Solida Sin.* 32 (5) (2019) 535–565.
- [5] K. Yu, T. Xie, J.S. Leng, Y.F. Ding, H.J. Qi, Mechanisms of multi-shape memory effects and associated energy release in shape memory polymers, *Soft Matter* 8 (2012) 5687–5695.
- [6] X.Z. Xin, L.W. Liu, Y.J. Liu, J.S. Leng, Origami-inspired self-deployment 4D printed honeycomb sandwich structure with large shape transformation, *Smart Mater. Struct.* 29 (6) (2020).
- [7] C. Lin, J.X. Lv, Y.S. Li, F.H. Zhang, J.R. Li, Y.J. Liu, L.W. Liu, J.S. Leng, 4D-Printed biodegradable and remotely controllable shape memory occlusion devices, *Adv. Funct. Mater.* 29 (51) (2019).
- [8] C. Lin, L. Liu, Y. Liu, J. Leng, The compatibility of polylactic acid and polybutylene succinate blends by molecular and mesoscopic dynamics, *Int J Smart Nano Mat* 11 (1) (2020) 24–37.
- [9] C. Lin, L.J. Zhang, Y.J. Liu, L.W. Liu, J.S. Leng, 4D printing of personalized shape memory polymer vascular stents with negative Poisson's ratio structure: a preliminary study, *Sci. China Technol. Sci.* 63 (4) (2020) 578–588.
- [10] T.Z. Liu, L.W. Liu, M. Yu, Q.F. Li, C.J. Zeng, X. Lan, Y.J. Liu, J.S. Leng, Integrative hinge based on shape memory polymer composites: material, design, properties and application, *Compos. Struct.* 206 (2018) 164–176.
- [11] F.F. Li, Y.J. Liu, J.S. Leng, Progress of shape memory polymers and their composites in aerospace applications, *Smart Mater. Struct.* 28 (10) (2019).
- [12] X. Guo, L. Liu, B. Zhou, Y. Liu, J. Leng, Constitutive model for shape memory polymer based on the viscoelasticity and phase transition theories, *J. Intell. Mater. Syst. Struct.* 27 (3) (2015) 314–323.
- [13] J.P. Gu, J.S. Leng, H.Y. Sun, H. Zeng, Z.B. Cai, Thermomechanical constitutive modeling of fiber reinforced shape memory polymer composites based on thermodynamics with internal state variables, *Mech. Mater.* 130 (2019) 9–19.
- [14] W. Zhao, L.W. Liu, J.S. Leng, Y.J. Liu, Thermo-mechanical behavior prediction of particulate reinforced shape memory polymer composite, *Compos. B Eng.* 179 (2019) 107455.
- [15] H. Zeng, N. Pan, J.P. Gu, H.Y. Sun, Modeling the thermoviscoelasticity of transversely isotropic shape memory polymer composites, *Smart Mater. Struct.* 29 (2) (2020).
- [16] C.X. Yin, H. Zeng, J.P. Gu, Z.M. Xie, H.Y. Sun, Modeling the thermomechanical behaviors of particle reinforced shape memory polymer composites, *Appl Phys Mater* 125 (6) (2019).
- [17] M.K. Hassanzadeh-Aghdam, M.J. Mahmoodei, Micromechanics-based characterization of elastic properties of shape memory polymer nanocomposites containing SiO<sub>2</sub> nanoparticles, *J. Intell. Mater. Syst. Struct.* 29 (11) (2018) 2392–2405.
- [18] R. Huang, S.J. Zheng, Z.S. Liu, T.Y. Ng, Recent advances of the constitutive models of smart materials - hydrogels and shape memory polymers, *Int J Appl Mech* 12 (2) (2020).

- [19] C.S. Jarali, M. Madhusudan, S. Vidyashankar, S. Raja, A new micromechanics approach to the application of Eshelby's equivalent inclusion method in three phase composites with shape memory polymer matrix, *Compos. B Eng.* 152 (2018) 17–30.
- [20] S.H. Nie, C. Basaran, A micromechanical model for effective elastic properties of particulate composites with imperfect interfacial bonds, *Int. J. Solid Struct.* 42 (14) (2005) 4179–4191.
- [21] A.S. Sangani, G.B. Mo, Elastic interactions in particulate composites with perfect as well as imperfect interfaces, *J. Mech. Phys. Solid.* 45 (11–12) (1997) 2001–2031.
- [22] Y.N. Rao, H.L. Dai, Micromechanics-based thermo-viscoelastic properties prediction of fiber reinforced polymers with graded interphases and slightly weakened interfaces, *Compos. Struct.* 168 (2017) 440–455.